Final manuscript accepted for publication in
Applied Radiation and Isotopes 165 (2020) 109259, pp 1-9

# Methods for the experimental study of $^{220}$Rn homogeneity in calibration chambers

**K. Mitev[a] , P. Cassette[b], D. Pressyanov[a], S. Georgiev[a], Ch. Dutsov[a], N. Michielsen[c], B. Sabot[b]**

[a] Sofia University "St. Kliment Ohridski", Faculty of Physics, 1164 Sofia, Bulgaria.
[b] CEA, LIST, Laboratoire National Henri Becquerel (LNE-LNHB), 91191 Gif-sur-Yvette Cedex, France.
[c] Institut de Radioprotection et de Sûreté Nucléaire (IRSN), 92262 Fontenay aux Roses, France.

**Abstract**
This work presents two experimental methods for the evaluation of $^{220}$Rn homogeneity in calibration chambers. The first method is based on LSC of the $^{220}$Rn decay products captured in silica aerogel. The second method is based on application of solid state nuclear track detectors facing the air of the calibration chambers. The performances of the two methods are evaluated by dedicated experiments. The repeatability of the method, estimated as relative standard deviation of the LSC measurements of ten silica aerogel samplers exposed under the same conditions is found to be 1.6%. Both methods are applied to study thoron homogeneity in the commercially available 50 L AlphaGuard emanation and calibration container, which was empty and its fan was turned on. It was found that the $^{220}$Rn distribution in this case is homogeneous within 10%. Both methods are also applied to test the thoron homogeneity in the BACCARA chamber at IRSN during a thoron calibration exercise. The results show that, at the centre of the chamber where the inputs of the sampling systems of the radon/thoron detectors were put close to each other, the thoron inhomogeneity is less than 10%. However, regions of higher thoron concentrations are clearly identified near the walls and the upper part of the chamber, with $^{220}$Rn concentrations being up to 60% higher compared to the concentration at the reference point. These results highlight the importance of the control and assessment of thoron homogeneity in thoron calibrations and in the cases when radon monitors are checked for thoron influence.

**Keywords:** Thoron ($^{220}$Rn), Thoron calibration, Thoron homogeneity, LSC, nuclear track detectors.

* Corresponding author.
*E-mail address:* kmitev@phys.uni-sofia.bg (K. Mitev).

https://doi.org/10.1016/j.apradiso.2020.109259
Received 27 March 2019; Received in revised form 28 April 2020; Accepted 1 June 2020
Available online 5 July 2020

## 1. Introduction

Thoron ($^{220}$Rn) is an isotope of the noble gas radon with 55.8 s half-life. Studies in the last decade demonstrate that doses from the thoron decay series cannot be considered negligible and there is a need for improvement of passive methods to measure thoron progeny and of the associated metrological assurance (McLaughlin, 2010; Hosodaet. al., 2017). The quality assurance of thoron measuring instruments and the studies of the influence of $^{220}$Rn on the radon measurement devices are areas of active research (Sabot et. al., 2016; Röttger et. al., 2009; Röttger et. al., 2010; Röttger et. al., 2014; Tokonami, 2005; He et. al., 2017; Michielsen and Bondiguel, 2015). However, the short half-life of $^{220}$Rn makes it difficult to ensure that it is homogeneously distributed in the chamber volume when thoron exposures are performed. Therefore, experimental methods able to probe thoron homogeneity are highly necessary.

The objective of this work is to present two newly proposed methods for evaluation of thoron homogeneity and their application in the thoron calibration exercise that has been carried out at IRSN in the framework of the MetroRADON Euramet EMPIR joint research project. The first method is based on a capture of thoron decay products in silica aerogel grains and subsequent liquid scintillation counting (LSC) of the silica aerogel. The second method is based on the measurement of the density of tracks formed by $^{220}$Rn and $^{216}$Po in Kodak Pathe LR-115/II solid state nuclear track detectors (SSNTDs). The two methods are applied successfully for the evaluation of $^{220}$Rn homogeneity in small (50 L) calibration vessels as well as in the BACCARA chamber (1 m$^3$) at IRSN with seven $^{220}$Rn measuring instruments inside.

## 2. Evaluation of thoron homogeneity by LSC of silica aerogel

This method makes use of a silica aerogel as thoron sampler and its subsequent mixing with a LS cocktail for LSC counting. The idea of the sampler is to allow thoron to enter freely from the environmental air into the cylindrical volume through the filters and to stop the thoron decay products on the filters. Thus, when $^{220}$Rn decays inside the sampler, its decay products ($^{216}$Po, $^{212}$Pb, $^{212}$Bi, $^{212}$Po and $^{208}$Tl) will attach to the silica aerogel and their activity in the silica aerogel will be proportional to the $^{220}$Rn activity that has entered in the cylinder. The latter is proportional to the ambient $^{220}$Rn activity concentration in the air surrounding the sampler. The usage of silica aerogel provides a large / sufficient amount of free space in the sampler for thoron to diffuse in and at the same time allows the effective capture of its decay products.

The $^{220}$Rn transport inside the sampler (assumed to have a cylindrical geometry) can be described by the diffusion equation with a term accounting for radioactive decay. As the thoron half-life is 55.8 s, for constant thoron concentration in the chamber and exposures longer than 10 min, a steady state diffusion can be assumed in the sampler:

$$D\frac{\partial^2 C}{\partial x^2} - \lambda C = \frac{\partial C}{\partial t}\ ,\ with\ \ \frac{\partial C}{\partial t} = 0 \qquad (1)$$

where $C$ is the $^{220}$Rn activity concentration, $D$ is the diffusion coefficient of $^{220}$Rn in the material, $\lambda$ is the $^{220}$Rn decay constant, $x$ is the space coordinate along the cylinder axis and $t$ is the time variable. The solution of the above equation in plate parallel geometry along the axis of the sampler is:

$$C(x) = C_{out}\frac{\cosh\left(\frac{2x-L}{2L_D}\right)}{\cosh\left(\frac{L}{2L_D}\right)} \quad (2)$$

and the $^{220}$Rn activity in the sampler ($A_{Tn}$) is given by

$$A_{Tn} = 2C_{out}V\frac{L_D}{L}\tanh\left(\frac{L}{2L_D}\right), \quad (3)$$

where $C_{out}$ is the outside $^{220}$Rn activity concentration (assuming that the filters are transparent to thoron), $L$ and $V$ are the height and the volume of the cylinder and $L_D=(D/\lambda)^{1/2}$ is the diffusion length of $^{220}$Rn in the material (air or silica aerogel, assuming that, due to the low-density of the aerogel, the diffusion within the aerogel is approximately the same as the diffusion in air). Taking into account that the diffusion coefficient of $^{220}$Rn in air is $D=10^{-5}$ m$^2$s$^{-1}$ (Ishimori et. al., 2013) which gives $L_D$=3.0 cm, from Eq. 2 it follows that one can expect non-homogeneous thoron distribution inside the sampler. Thus, it is important, as shown hereafter, to choose carefully the thickness of the samplers to ensure best performance.

Specially designed thoron samplers were developed as shown in Fig 1. The sampler consists of a cylindrical body and two end caps, which serve to fix and support two air filters (bottom and top) at the ends of the cylinder (Fig. 1a). The inner and the outer diameters of the cylinder are 4.4 cm and 4.7 cm, respectively. The diameters were chosen to fit the diameter of the filters (d=4.7 cm). The silica aerogel used in this work is commercially available from various producers and is used for cat litters. It was crushed and sieved (from ~0.5 mm to 3.0 mm) to get grains with suitable size – small enough so they can fit in the sampler without punctuating the closing filters and, at the same time, large enough (e.g. larger than dust particles) to allow the aerogel to absorb the LS cocktail quickly in order to perform the LSC measurement as soon as possible after the exposure. The silica is placed in the cylinder (Fig. 1b) and the sampler is closed tight (Fig. 1c). All plastic parts of the thoron sampler are locally made with a 3D printer.

In order to evaluate the thoron homogeneity during the calibration exposures the thoron samplers can be positioned at any point of interest in the calibration chamber. After the end of the thoron exposure, the samplers are removed and the silica aerogel from each sampler is carefully transferred into a LS glass vial (high performance glass vials by Perkin Elmer were used in this work). The mass of the transferred silica aerogel is determined by weighing the LS vials. The vials are then filled with 15 mL Ultima Gold LLT LS cocktail and placed for 10 min in an ultrasonic bath in order to facilitate the full penetration of the scintillation cocktail in the silica aerogel and to remove air bubbles from it (Fig. 3).

Different types of filters were tested - glass microfiber filter with an equivalent pore size of 1.2 μm and thickness 260 μm (LLG-Labware 9045867), mixed cellulose ester membrane filter with an equivalent pore size of 0.2 μm and thickness 130 μm (ADVANTEC A20A047A) and mixed cellulose ester membrane filter with 0.3 μm equivalent pore size and thickness 150 μm (Millipore PHWP04700). The performance criterion for the choice of the filter is the agreement between the measured net LS counting rate and the expected net LS counting rate from the activity, absorbed in the aerogel, which is determined from Eq. 3.

The results from the tests showed that net LS counting rate obtained with the glass microfiber filters is always higher than the net LS counting rate expected from the absorbed activity (Eq. 3). Therefore, we conclude that the used glass microfiber filters do not completely stop the thoron progeny from penetrating in the samplers. The best agreement between the measured and the expected net LS counting rate was obtained with two membrane filters placed on each entry of the sampler. Both types

of filters ADVANTEC A20A047A and Millipore PHWP04700 show excellent performance. Scanning electron microscope images of the used membrane filters are shown in Fig. 2.

In order to choose the optimal thickness, three different samplers were produced with L=1.0 cm, 1.5 cm and 2.0 cm. Six samplers (two of each thickness) were exposed to thoron in a 50 L AlphaGuard calibration container with an AlphaGuard PQ2000 PRO (Rn/Tn) reference monitor placed inside. The AlphaGuard PQ2000 PRO (Rn/Tn) reference monitor is used with its factory calibration for $^{220}$Rn (Saphymo, Germany). The $^{220}$Rn activity concentration during the exposure was $C_{out}$=612(61) kBq m$^{-3}$ and the exposure duration was 68.2 h. The samplers were placed at the bottom of the vessel close to each other with a special focus on $^{220}$Rn freely reaching each sampler and passing through the filters. After the exposure the silica aerogel from each sampler was transferred into a high-performance glass vial and the vials were measured on a RackBeta 1219 LS counter (Wallac, Finland). The results are shown in Table 1 and indicate that the thinnest samples have the highest net counting rate per unit mass. Considering the results in Table 1 and noting that the net LS counting rate is due to several thoron progenies ($^{212}$Pb, $^{212}$Bi , $^{212}$Po and $^{208}$Tl) it can be concluded that samplers with thickness $L$=1 cm which contain around 5 g of silica aerogel provide sufficiently good sensitivity for the method to be applied for the evaluation of $^{220}$Rn homogeneity.

The most important characteristic of the proposed method from the point of view of practical applications is its repeatability. It is studied in this work with the experimental set-up shown schematically in Fig. 4 and on the photo in Fig. 5. The set-up consists of a powerful fan (gas-flow 2.5 m$^3$ min$^{-1}$) mounted to a tube. Inside the tube there are 10 thoron samplers divided in two groups (AG1 to AG5 mounted closer to the fan and AG6 to AG10 just behind them, see Fig. 4a and Fig 5a). The samplers are positioned with their filter-sides parallel to the air-flow (see Fig. 4b and Fig 5b). The entire system is placed in a 50 L calibration container (Fig. 6) with one thoron sampler placed at the exit of the tube perpendicular to the gas–flow (AG11) and another sampler placed outside beside the tube (AG12), see Fig. 4a and Fig. 6. The thoron inlet is positioned right in front of the fan and the container is closed hermetically. The gas-flow of the fan (150 m$^3$ h$^{-1}$) is chosen large enough to guarantee that all the samplers in the tube (AG1-AG10) are exposed to the same thoron concentration and the volume refresh rate (50 times per min) is sufficient to assume that AG11 and AG12 are also exposed to the same concentration. The duration of the $^{220}$Rn exposure was 66 h and the thoron activity concentration in the container was 474(47) kBq m$^{-3}$. After the exposure, the silica aerogel from the samplers was transferred and measured on the RackBeta 1219 LS counter as described above. The net counting rate of each sample was followed for 60 h and the net counting rates at the moment of the end of exposure are evaluated. The results, presented in Table 2, show that the relative standard deviation of the net counting rates per unit mass of the samplers in the tube (AG1-AG10) is 1.6% and their variations are fully within the estimated uncertainties. Moreover, the sampler AG11, which is in front of the tube and is perpendicular to the air stream also agrees well with the mean value within its estimated uncertainty. The same is also true for the sampler AG12, which is behind the tube (see Fig. 4a and Fig. 6). These results suggest a repeatability of the method of the order of 1.6%, which is an excellent repeatability for the evaluation of thoron homogeneity in $^{220}$Rn calibrations.

## 3. Evaluation of thoron homogeneity by SSNTDs

The other approach we investigated to evaluate the homogeneity of $^{220}$Rn in chambers is based on the use of bare SSNTDs, placed at different points inside the chamber. These detectors register alpha particles that reach the detector surface with energy and incident angle within certain registration window specific for each type of SSNTDs. Normally, the air contains a mixture of isotopes (in this case $^{220}$Rn and its progeny atoms $^{216}$Po, $^{212}$Pb, $^{212}$Bi+$^{212}$Po/$^{208}$Tl, $^{212}$Po is always in equilibrium with $^{212}$Bi). However, in an exposure chamber volume a substantial part of the progeny atoms is deposited on the internal walls (George et al., 1983). The deposited fraction is higher when a fan creates air turbulence inside the chamber (Cheng et al., 1990). For instance, the deposited fractions of $^{222}$Rn progeny in a 200 L spherical volume with a fan operating inside have been evaluated experimentally in the past (Pressyanov, 2002): Within this experiment $^{222}$Rn was injected in the closed 200 L volume. After initially pure $^{222}$Rn is injected, its progeny starts to grow, reaching after 4-5 hours a radioactive equilibrium with $^{222}$Rn. Under equilibrium the activity of each of its progeny isotopes $^{218}$Po, $^{214}$Pb and $^{214}$Bi ($^{214}$Po is always in equilibrium with $^{214}$Bi) is equal to that of $^{222}$Rn. While the $^{222}$Rn atoms are only in the air, those of its progeny are either in the air or deposited on the internal surface of the volume. The fractions of the individual $^{222}$Rn progeny isotopes in air were estimated by parallel measurements (after an equilibrium is reached) of the activity concentrations of $^{222}$Rn, $^{218}$Po, $^{214}$Pb and $^{214}$Bi. The air fraction of a particular isotope is the ratio of its activity concentration to that of $^{222}$Rn and the deposited fraction is what remains up to 100%. In this experiment the deposited fractions were estimated to be 94.0%, 99.7% and 99.9% for $^{218}$Po (half-life 3.05 min), $^{214}$Pb (half-life 26.8 min) and $^{214}$Bi (half-life 19.9 min), respectively. When $^{220}$Rn + progeny is created in the chamber, due to the longer half-life of $^{212}$Pb (half-life 10.64 h) and $^{212}$Bi (half-life 60.55 min) one can expect that practically all of the $^{212}$Pb and $^{212}$Bi+$^{212}$Po atoms are deposited on the walls and their air fraction is negligible. Results of other authors (Harley et. al., 2010) also show extreme disequilibrium in air between $^{220}$Rn and its decay products $^{212}$Pb and $^{212}$Bi, even for much larger volumes (e.g. rooms) than the volumes of 200 L or 1 m$^3$. Therefore, within the present approach, we assume that the isotopes in the air are $^{220}$Rn and $^{216}$Po and that $^{216}$Po, due to its short half-life of 0.15 s, has of the same volume distribution as $^{220}$Rn.

In our experiments SSNTDs of Kodak-Pathe LR-115 type II were used. They register alpha particles within an energy and angular window of registration that depends on the etching conditions and the mode of counting. These conditions in our case were etching with 10% NaOH at 60 $^0$C for 100 min, washing with water for 30 min and washing for 2 min in still 50% ethanol and visual counting by microscope - only of tracks that created holes through the 12 μm sensitive layer of this type of detectors were counted. As described elsewhere (Pressyanov, 2012), under these conditions the detectors register alpha particles of energy within 1.5 – 4.0 MeV and incident angle <55$^o$ to the normal. The air volumes from which the alpha particles of different isotopes can be detected are schematically shown in Fig.7. What is essential for this application is that the alpha particles from the $^{220}$Rn progeny atoms deposited on the detector surface cannot be detected, as their energy is well above the upper energy threshold of the window for registration. From Fig.7 it follows that, to avoid contribution from the atoms deposited on the chamber internal surface, the SSNTD face should look to air being at a distance of at least 8 cm from any surface – i.e. outside the range of $^{212}$Po alphas. Under these conditions the tracks will be due only to

the alpha particles from the sources in the air ($^{220}$Rn and $^{216}$Po) and the registered tracks will originate from the isotopes that are in a small volume within a distance of 2.4 – 5.0 cm from the detector surface ("detection volumes", see Fig. 7).

Respecting the above rule, Kodak-Pathe LR-115/II detectors were used in two experiments. The first was in 50 L cylindrical exposure chamber in which 33 SSNTDs were placed. The map of the "detection volumes" is shown in Fig. 8. The exposure was made at the laboratory facility, described elsewhere (Pressyanov et. al., 2017). The exposure was made at an average $^{220}$Rn concentration of 800(50) kBq m$^{-3}$ for 220 min. During exposure a fan worked continuously in the chamber and the $^{220}$Rn concentrations were followed by a reference instrument AlphaGUARD PQ2000 PRO (Rn/Tn). The analysis of the results showed that the distribution of $^{220}$Rn in the air is homogeneous within about 10% (Fig. 9). The variations between the results can be explained by the detector reading uncertainty and sub-volumes of significantly higher or lower concentrations cannot be identified. Similar homogeneity (i.e. within 10%) of the empty 50 L AlphaGuard calibration volume with its own fan turned on is obtained by the LS counting of the silica aerogel (not shown).

## 4. Application of the methods during the thoron calibration exercise, performed at BACCARA chamber at IRSN

A thoron calibration exercise was carried out in May 2018 in the framework of the MetroRADON Euramet project using the IRSN reference radon chamber called BACCARA. The BACCARA chamber is a 1 m$^3$ stainless steel chamber with a thoron reference instrument attached to it (Sabot et. al., 2016), which is used to create reference radon and thoron atmospheres for calibration of radon and thoron measuring devices. During the thoron calibration exercise, four AlphaGuards and three RAD7 instruments were placed in the chamber and their thoron measurement performance was checked against the reference instrument (Fig. 10). The thoron calibration exercise and its results will be described in detail elsewhere. In order to test the thoron homogeneity in the BACCARA chamber during the calibration exercise12 silica aerogel thoron samplers and 22 SSNTDs were placed at different positions in the chamber (Fig. 10). The SSNTDs were placed in all parts of BACCARA internal volume, but respecting the stated above rule for detector positioning. The thoron exposure duration was 48 h and the $^{220}$Rn activity concentration in the chamber was 46 kBq m$^{-3}$. In order to avoid the effect of possible $^{220}$Rn inhomogeneity during the calibration, the inputs of the instruments sampling systems were put close to each other as much as possible to the extent of forming a sampling point in the chamber (Fig. 11). The silica aerogel samples and the SSNTDs were placed around the sampling and all other parts of the chamber, trying to cover the upper part of the chamber (Figures 12 and 13) as well as the space around the sampling points and around and between the detectors (Fig. 14).

After the end of the exposure, the silica aerogel samples were treated as described above. The activity in the samples is measured on a Wallac Guardian LS counter at LNHB and the results are shown in Table 3. For better visualization, the values obtained with the different samplers are shown relative to the reference point in Figures 11-14. The results in Table 3 and Fig. 11 show that the differences between the $^{220}$Rn concentrations in positions "C", near the center of the chamber, close to the instruments' sampling points, do not exceed 10%. But, one can observe higher differences for positions "W", far from the center of the chamber, for example the $^{220}$Rn concentrations near the upper wall of the chamber (AT7) are up to 61% higher than those in the center (Fig. 12). Similarly, the thoron concentration near the walls of

the chamber are higher than those at the reference point (see, for example AT4, AT5, AT11 and AT7 in Fig. 12 and 13). The $^{220}$Rn concentration below the instruments (AT8) are also higher than those in the reference point (Fig. 14). Overall, it seems that the $^{220}$Rn concentration near the sampling point of the instruments is homogeneous, but there are volumes in the chamber near the walls, the entry point of the thoron and in front of the fan where much higher $^{220}$Rn concentrations are observed.

The SSNTD results reveal signs of inhomogeneity with up to about 60% deviation from the reference point (Fig. 15). It should be noted also that the silica aerogel sampling method and the SSNTD method give consistent results for the points where the two methods can be applied (see Fig. 13). For example, the detection volume of the highest deviation ratio 1.61(0.18) corresponds to SSNTD No 4 and it is close to the space where LSC of silica aerogel (AT5) also showed high deviation (ratio of 1.55). Similarly, SSNTD No 7 and AT11, which are close at the back of the chamber, give very close results (Fig. 13). The two methods clearly demonstrate that there can be high thoron inhomogeneity near the walls of the chamber.

## 5. Conclusions

Two experimental methods for evaluation of $^{220}$Rn homogeneity in calibration chambers are presented. The first method is based on LSC of thoron short-lived decay products captured in silica aerogel and the second method is based on application of SSNTDs. The performance of the two methods is evaluated in several dedicated experiments where it is shown that the repeatability of the method based on LSC of silica aerogel is within 1.6%. Both methods are applied to study thoron homogeneity in a 50 L empty AlphaGuard emanation and calibration container with its fan turned on, and it was found that thoron distribution is homogeneous within 10%.

Both methods are applied successfully to test the thoron homogeneity in the BACCARA chamber during the thoron calibration exercise that was carried out at IRSN, France in the framework of the MetroRADON Euramet EMPIR project. The results show that, at the centre of the chamber, where the inputs of the instruments sampling systems were put close to each other, the thoron inhomogeneity is less than 10%. However, regions of higher thoron concentrations are clearly identified near the walls and the upper part of BACCARA, with $^{220}$Rn concentrations being up to 60% higher compared to the concentration at the reference point. These results highlight the importance of the control and assessment of thoron homogeneity in thoron calibrations and in the case when radon monitors are checked for thoron influence. The assessment of $^{220}$Rn homogeneity will be particularly important in the case of checking passive radon monitors for thoron influence. That is because, contrary to the case of active monitors, there are no inputs of the passive detectors, so they cannot be put together near a common sampling point in the calibration chamber. Thus, an experimental method for checking thoron homogeneity as those described in this work will be highly necessary.

**Acknowledgements**

This work is supported by the European Metrology Programme for Innovation and Research (EMPIR), JRP-Contract 16ENV10 MetroRADON (www.euramet.org). The EMPIR initiative is co-funded by the European Union's Horizon 2020 research and innovation programme and the EMPIR Participating States.

## References


Cheng, Y. S., Su, Y. F., Chen, B. T., 1990. Plate-out rates of radon progeny and particles in a spherical chamber. Proc. XXIX Hanford Symposium on Health and the Environment, pp. 65-79.

George, A. C., Knutson, E. O., Tu, K. W., 1983. Radon daughter plateout – I measurements. Health Phys. 45, 439-444.

Harley, N., Chitaporn, P., Medora, R., Merrill, R., 2010. Measurement of the indoor and outdoor $^{220}$Rn (thoron) equilibrium factor: Application to lung dose. Radiat. Prot. Dosimetry 141, 357-362.

He, Z., Xiao, D., Lv, L., Zhou, Q., Wu, X., Shan, J., 2017. Stable control of thoron progeny concentration in a thoron chamber for calibration of active sampling monitors, Radiation Measurements. 102, 27-33.

Hosoda, M., Kudo, K., Iwaoka, K., Yamada, R., Suzuki, T., Tamakuma, Y., Tokonami, S., 2017. Characteristic of thoron ($^{220}$Rn) in environment, Appl. Radiat. Isot. 120, 7-10.

Ishimori,Y., Lange, K., Martin. P., Mayya, Y.S., Phaneuf, M., 2013. Measurement and calculation of radon releases from NORM residues, IAEA technical reports series No. 474.

Kobayashi, Y., Tokonami, S., Takahashi, H., Zhuo, W., Yonehara, H., 2005. International Congress Series, 1276, 281-282.

McLaughlin, J., 2010. An overview of thoron and its progeny in the indoor environment, Radiat. Prot. Dosimetry. 141, 316-321.

Michielsen, N., Bondiguel, S., 2015. The influence of thoron on instruments measuring radon activity concentration, Radiat. Prot. Dosimetry. 141, 289-292.

Pressyanov, D., 2002. Evaluation of the radiological hazards in houses and working places by integrated measurements of the individual $^{222}$Rn progeny in air. Research contract between the Ghent University and Sofia University "St. Kliment Ohridski" (DOB/HB/RS/02), final report.

Pressyanov. D, 2012. Radon and Radon Progeny: Methodological Points and Case Studies. Lambert Academic Publishing GmbH & Co. KG, Saarbruecken, Germany. ISBN: 978-3-8484-8604-5

Pressyanov D., Mitev K., Georgiev S., Dimitrova I., Kolev J. (2017) Laboratory facility to create reference radon + thoron atmosphere under dynamic exposure conditions. J. Env. Radioact.166, 181-187.

Röttger, A., Honig, A., Arnold, D., 2009. The German thoron progeny chamber – Concept and application, Appl. Radiat. Isot. 67, 839-842.

Röttger, A., Honig, A., Dersch, R., Ott, O., Arnold, D., 2010. A primary standard for activity concentration of $^{220}$Rn (thoron) in air, Appl. Radiat. Isot. 68, 1292-1296.

Röttger, A., Honig, A., Linzmaier, D., 2014. Calibration of commercial radon and thoron monitors at stable activity concentrations, Appl. Radiat. Isot. 87, 44-47.

Sabot, B., Pierre, S., Michielsen, N., Bondiguel, S., Cassette, P., 2016. A new thoron atmosphere reference measurement system, Appl. Radiat. Isot. 109, 205-209.

# Figures

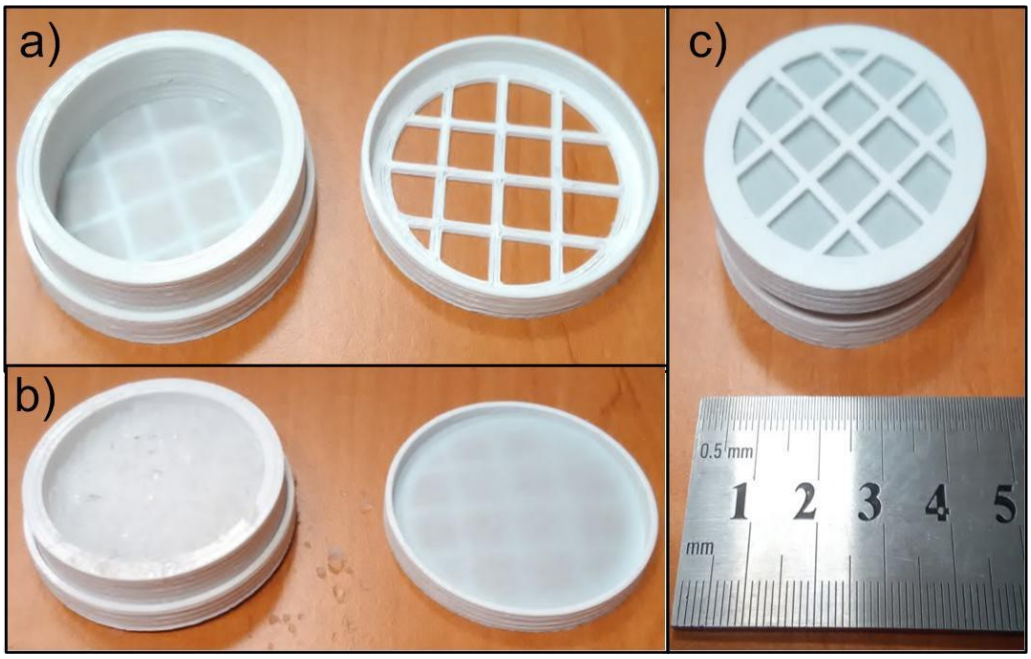


Fig. 1. A photograph of a thoron sampler. a) – Empty sampler, with bottom air filter, ready to be filled with silica aerogel and the top end cap with top air filter mounted; b) the sampler filled with silica aerogel; c) closed sampler ready to be placed in thoron chamber.

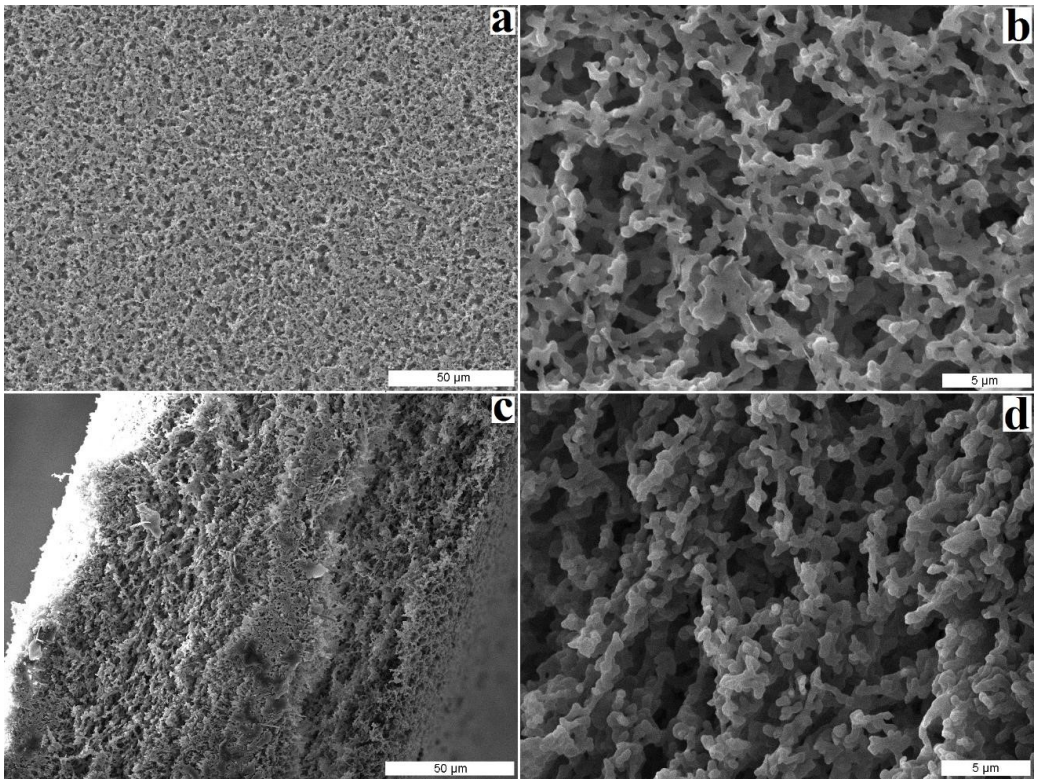


Fig. 2. Scanning electron microscope images of the Millipore membrane filters used for the samplers. a) and b) –surface view, c) and d) – cross-sectional view.

Fig. 3. High performance LS glass vials (20 ml) filled with silica aerogel and Ultima Gold LLT LS cocktail. The photograph is taken after the vials had been placed for 10 min in a ultrasonic bath. When filled with LSC cocktail, the aerogel becomes translucent.

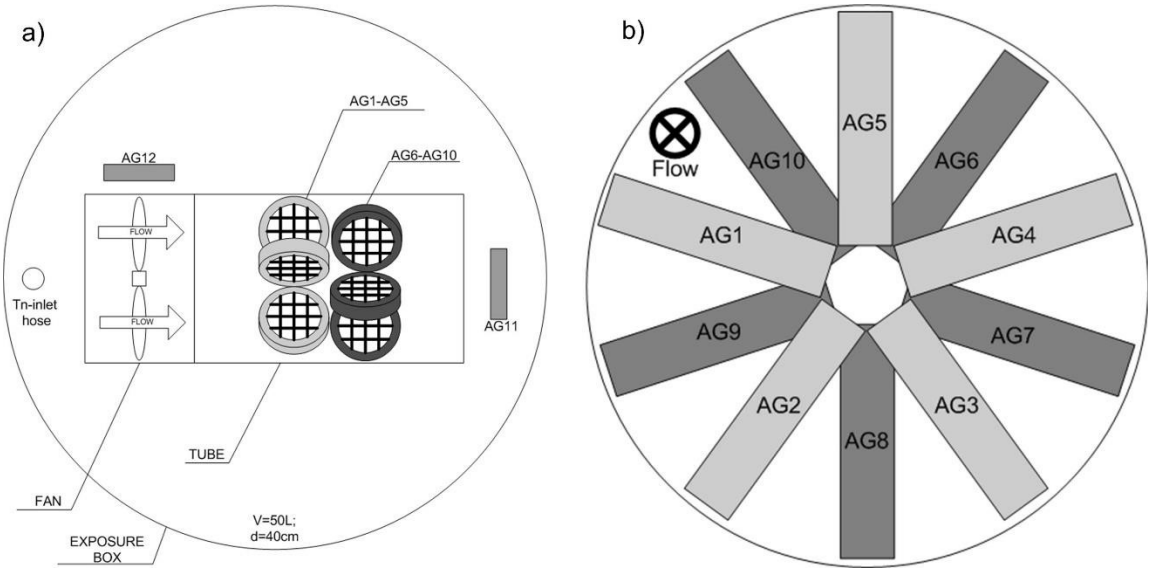


Fig. 4. Schematic view of the geometry used to test the repeatability of the silica aerogel method. a) Schematic view of the exposure vessel, the $^{220}$Rn inlet, the fan and the tube with the thoron samplers; b) Illustration of the arrangement of the thoron samplers in the tube.


Fig. 5. Photographs of the experimental arrangement used to test the repeatability of the silica aerogel method: the fan, the tube and the thoron samplers can be seen in the picture.

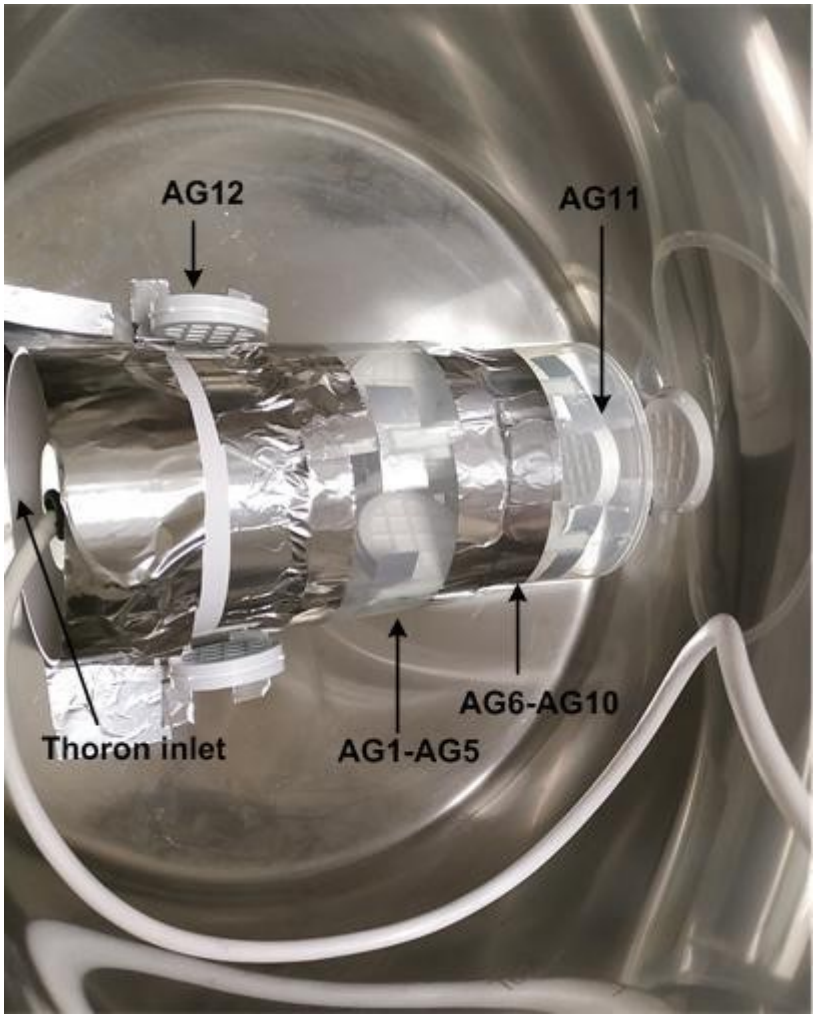


Fig. 6. Photograph of the exposure set-up used to test the repeatability of the silica aerogel method. The fan and the tube with the samplers are placed in a 50 L vessel. Additional samplers are placed in front and near the tube.

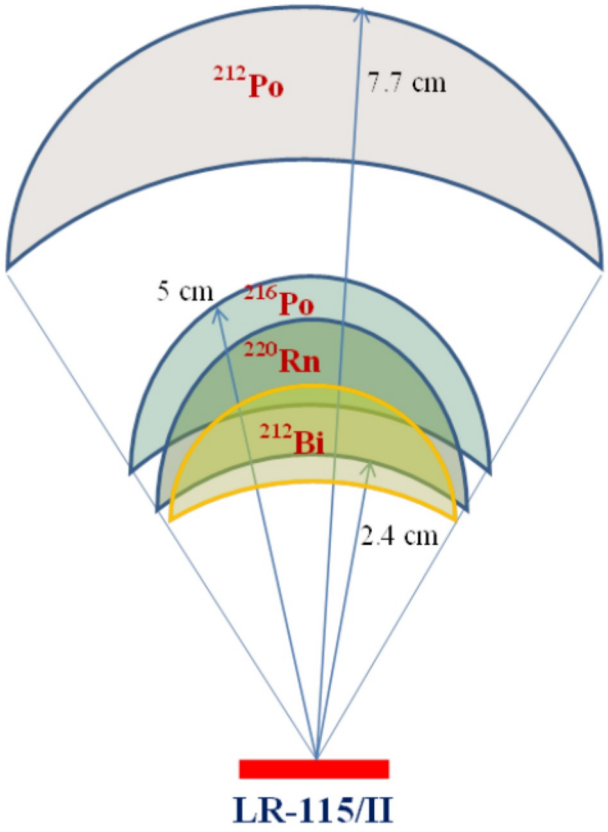


Fig. 7. Air-volumes from which alpha particles can be detected by LR-115/II SSNTD. The volumes are shaped taking into account the fact that energy window for track registration get narrow when the incident angle is increasing.

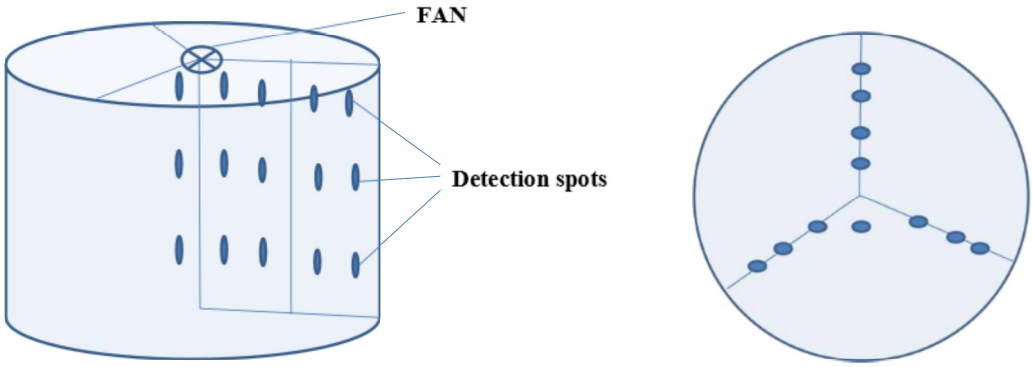


Fig. 8. The picture shows the spots in the chamber volume from where activity can be detected by the placed in a grid Kodak Pathe LR-115/II SSNTD ("detection" volumes).

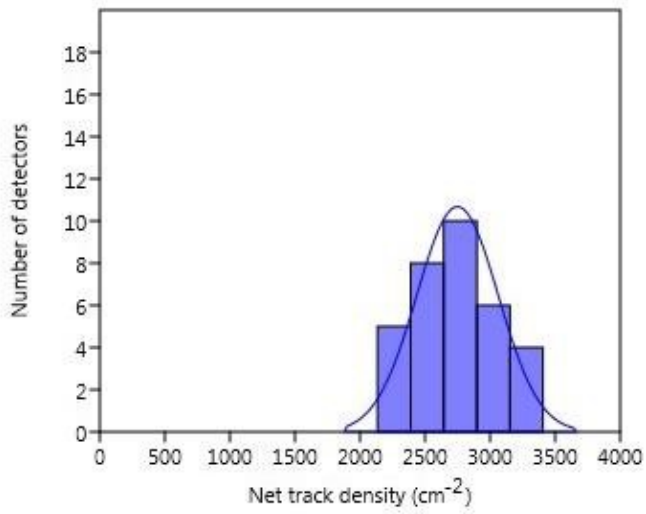


Fig. 9. Distribution of the net track density from the exposed SSNTDs. The net track density is the track density after the background of not exposed detectors (16 ± 3 $cm^{-2}$) is subtracted. The curve is the gaussian distribution fit which standard deviation is 10% of the mean.

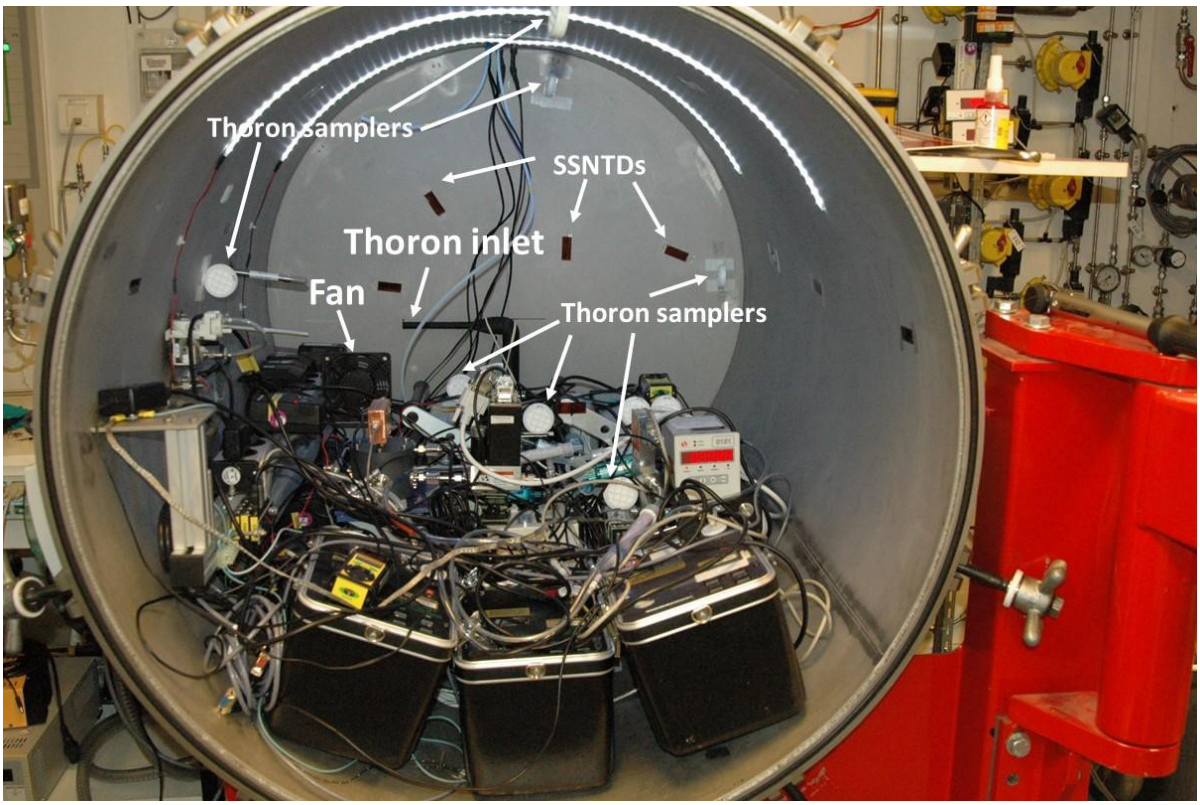


Fig. 10. A photograph of the BACCARA chamber showing the experimental set-up used in the thoron calibration exercise. The thoron inlet nozzle and the fan used to homogenize the air in the chamber are indicated as well as the positions of some of the thoron samplers and the SSNTDs.

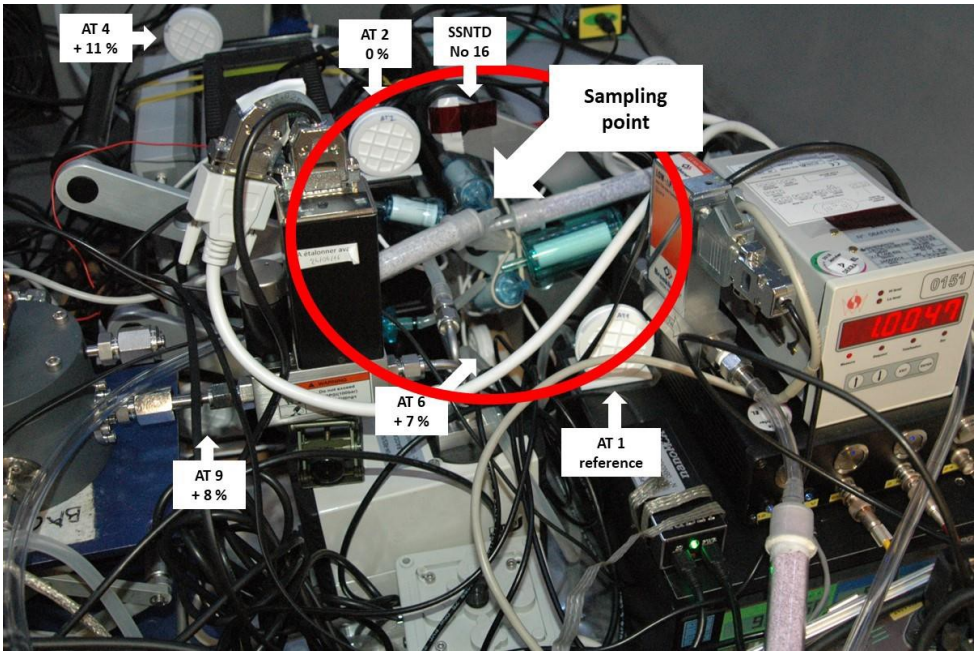


Fig. 11. Photograph showing the sampling point, where the inlets of the thoron measuring instruments are located. There are thoron samplers (AT1, AT2 and AT6) and a SSNTD (No 16) around the sampling point. The percent in the boxes with the sampler number indicate the sampler's readings relative deviation with respect to the reference (AT1).

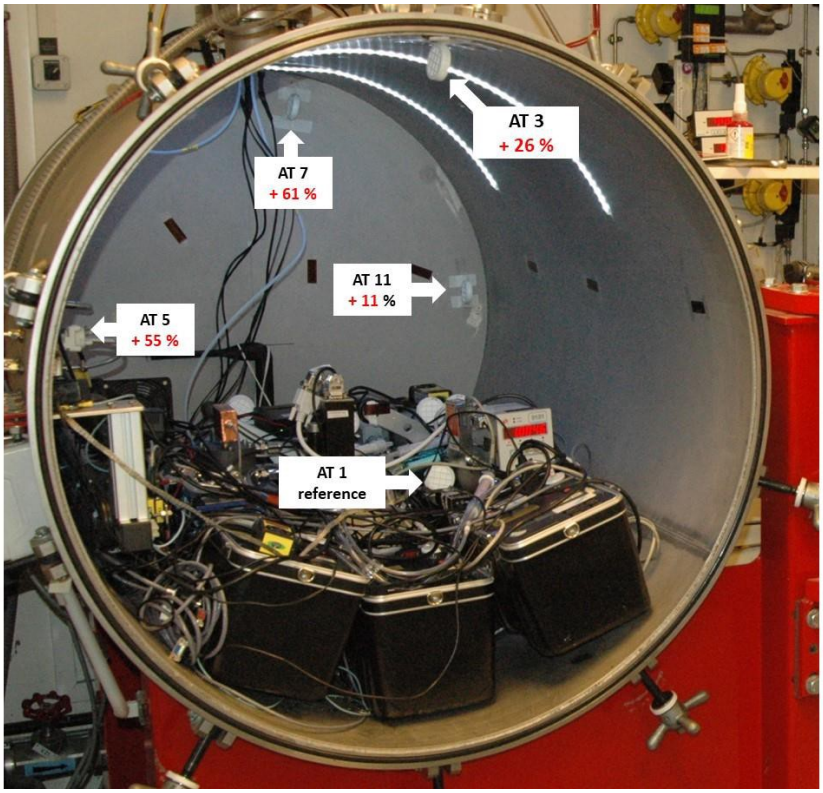


Fig. 12. Position and relative deviation with respect to the reference position of the readings of the thoron samplers in the upper half of the BACCARA.

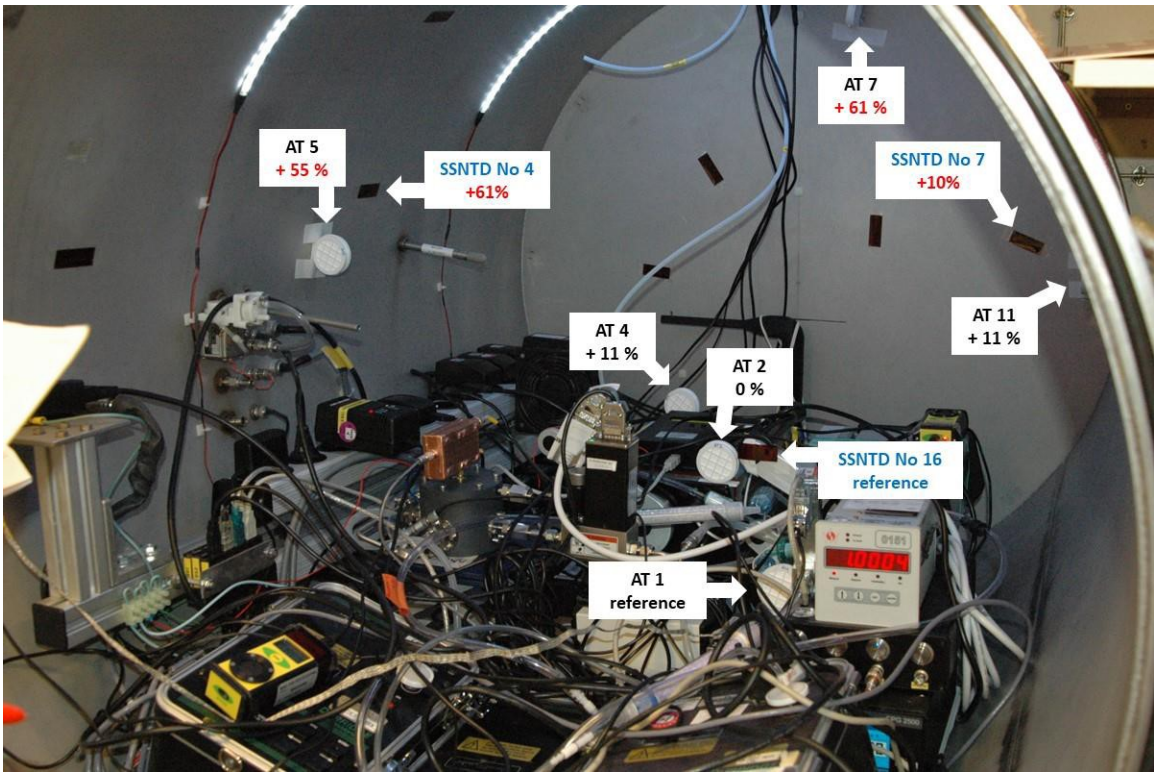


Fig. 13. Position and relative deviation with respect to the reference position of the readings of the thoron samplers in the upper half of the BACCARA and near the sampling point.

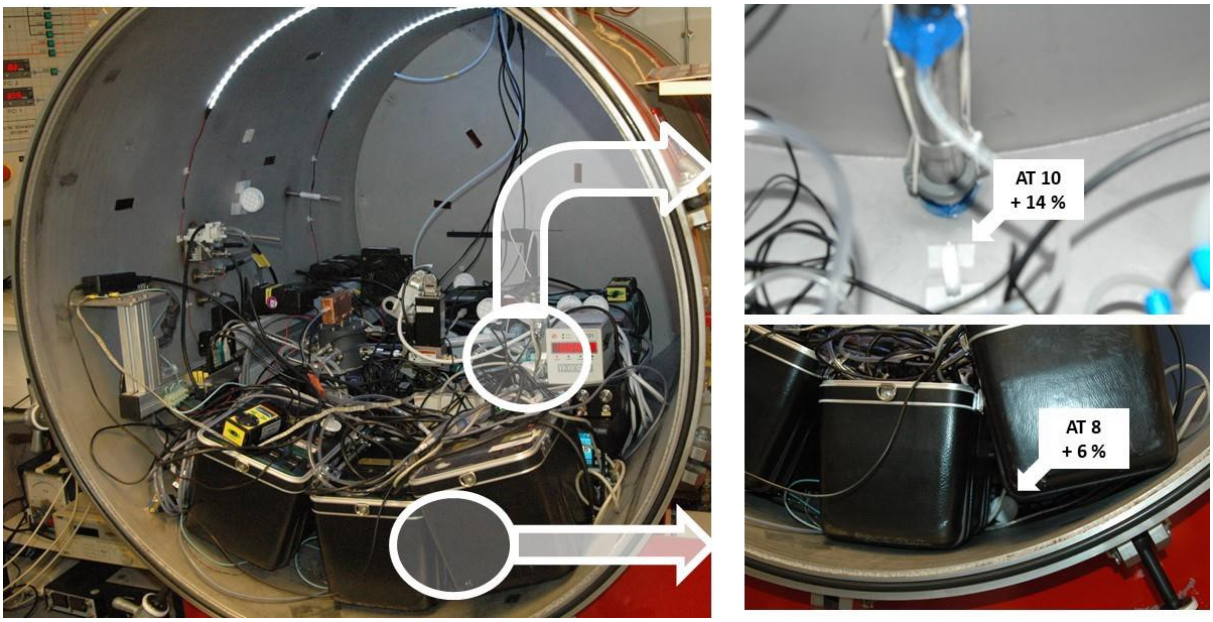


Fig. 14. Position and relative deviation with respect to the reference position of the readings of the thoron samplers located below and between the $^{220}$Rn measuring instruments.

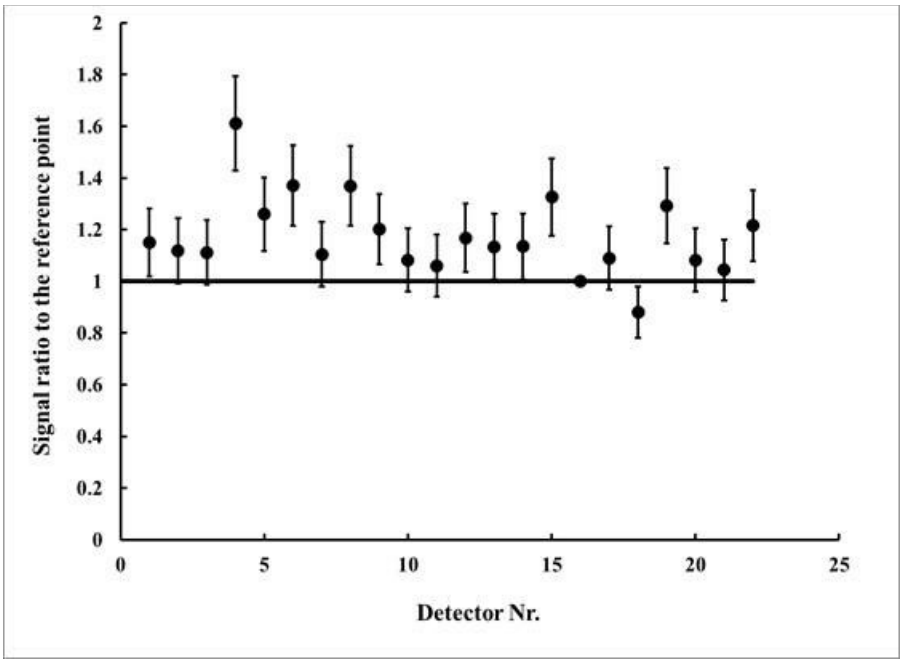


Fig. 15. The ratio of the SSNTD signal (net track density) to the signal of the detector that is at closest distance to the reference point (detector No 16).

## TABLES

**Table 1:** Net counting rates per unit mass of thoron samplers with different heights exposed together to $^{220}Rn$ in air.

| Sampler | L, cm | V, $cm^3$ | Mass of the silica aerogel in the samplers, g | Net LS counting rate per unit mass of the silica aerogel, $s^{-1}g^{-1}$ |
|---|---|---|---|---|
| S1 | 1.0 | 15.21 | 5.421(5) | 10.290(58) |
| S2 | 1.0 | 15.21 | 5.202(5) | 10.415(60) |
| M1 | 1.5 | 22.81 | 8.649(5) | 9.119(56) |
| M2 | 1.5 | 22.81 | 8.472(5) | 9.054(58) |
| L1 | 2.0 | 30.41 | 11.932(5) | 7.761(56) |
| L2 | 2.0 | 30.41 | 11.920(5) | 7.714(55) |

**Table 2:** Study of the repeatability of $^{220}$Rn readings with thoron samplers. The numbers in the brackets indicate the overall estimated standard uncertainties.

| Thoron sampler | Mass of the silica aerogel in the LS vial (g) | Net LS counting rate per unit mass of the silica aerogel at the end of the exposure($s^{-1}g^{-1}$) | Difference from the mean (%) |
|---|---|---|---|
| AG 1 | 5.014(5) | 6.44(26) | 1.3% |
| AG 2 | 5.064(5) | 6.24(22) | -1.9% |
| AG 3 | 5.054(5) | 6.40(14) | 0.6% |
| AG 4 | 4.914(5) | 6.31(16) | -0.8% |
| AG 5 | 5.055(5) | 6.43(16) | 1.0% |
| AG 6 | 5.050(5) | 6.51(18) | 2.3% |
| AG 7 | 5.040(5) | 6.21(21) | -2.3% |
| AG 8 | 5.042(5) | 6.26(12) | -1.6% |
| AG 9 | 5.043(5) | 6.37(19) | 0.1% |
| AG 10 | 5.021(5) | 6.44(20) | 1.3% |
| AG 11 | 5.062(5) | 6.48(25) | 1.8% |
| AG 12 | 4.884(5) | 6.22(14) | -2.2% |
| mean AG1-AG10 $x$ | 5.030 | 6.36 | |
| std. dev. $s$ | 0.059 | 0.10 | |
| $u_{bb}$ = rel. std. dev. $s/x$ (%) | 1.2 % | 1.6 % | |

**Table 3:** Homogeneity study with thoron samplers during the thoron calibration exercise performed in the BACCARRA chamber. The numbers in the brackets indicate the overall estimated standard uncertainties.

| Sample | Decay corrected net counting rate, cpm | Mass of the silica aerogel in the LS vial (g) | Specific net LS counting rate at the end of the exposure($s^{-1}g^{-1}$) | Center (C) / Walls (W) | Normalized to AT1 |
|---|---|---|---|---|---|
| AT1 | 108.2(17) | 5.346(5) | 20.24(32) | C | 1.00 |
| AT2 | 111.9(18) | 5.546(5) | 20.17(33) | C | 1.00 |
| AT3 | 139.1(20) | 5.444(5) | 25.56(37) | W | 1.26 |
| AT4 | 122.6(20) | 5.471(5) | 22.41(37) | C | 1.11 |
| AT5 | 169.6(24) | 5.402(5) | 31.39(44) | W | 1.55 |
| AT6 | 116.2(22) | 5.361(5) | 21.68(41) | C | 1.07 |
| AT7 | 179.2(26) | 5.503(5) | 32.57(48) | W | 1.61 |
| AT8 | 119.6(24) | 5.550(5) | 21.54(44) | W | 1.06 |
| AT9 | 119.5(26) | 5.454(5) | 21.91(47) | C | 1.08 |
| AT10 | 127.7(27) | 5.550(5) | 23.00(50) | C | 1.14 |
| AT11 | 125.8(29) | 5.598(5) | 22.47(51) | W | 1.11 |